Journal of Biomolecular NMR, 3 (1993) 653–673
ESCOM

J-Bio NMR 142

Oxytocin solution structure changes upon protonation of the N-terminus in dimethyl sulfoxide

Toshiyo Kato[a], Shigeru Endo[b], Toshimichi Fujiwara[a,*] and Kuniaki Nagayama[a,**]

[a]*Biometrology Laboratory, JEOL Ltd., 3-1-2 Musashinocho, Akishima, Tokyo 196, Japan*
[b]*Protein Array Project, ERATO, JRDC, 5-9 Tokodai, Tsukuba 300-26, Japan*

Received 8 December 1992
Accepted 25 June 1993

Keywords: ^{1}H NMR; ^{13}C NMR; Oxytocin; Assignment; Solution structure

SUMMARY

With the combined use of various two-dimensional (2D) NMR techniques, a complete assignment of the ^{1}H and ^{13}C resonances of oxytocin, Cys-Tyr-Ile-Gln-Asn-Cys-Pro-Leu-Gly-NH_2, for two molecular states, protonated and unprotonated at the N-terminal group, was performed in dimethyl sulfoxide. A small but distinct change in the backbone conformation of the six-residue cyclic moiety, associated with the protonation, was first suggested from those NMR parameters relevant to conformation, such as change with temperature in the chemical shifts of the peptide amide protons and changes in chemical shifts and homonuclear as well as heteronuclear three-bond coupling constants. The solution structures of oxytocin for the protonated and unprotonated forms were then calculated using distance analysis in dihedral-angle space, based on a relaxation matrix evaluated from quantitative NOE intensities at different mixing times. Total amounts of 93 and 105 distances were determined for the protonated and the unprotonated forms, respectively. There were 25 interresidue distances relevant to the structure of the cyclic moiety for the protonated form of oxytocin and 43 for the unprotonated form. Overall structures with the lowest target penalty function were similar between the two forms, having a β-turn structure at the endocyclic residues of the Tyr-Ile-Gln-Asn moiety. The local backbone conformations near the N-terminus, however, were significantly different between the two forms. This was found to be due to a change in the dihedral angle of the disulfide bridge (χ^{ss} around C-S-S-C), which closes the ring in the cyclic peptide. The dihedral angle was about +90° for the unprotonated form and an intermediate value of about +45° for the protonated form.

INTRODUCTION

Oxytocin, Cys-Tyr-Ile-Gln-Asn-Cys-Pro-Leu-Gly-NH_2 (MW about 1000), is a neurohypophyseal peptide hormone with major physiological activities in milk ejection and uterine contrac-

*Present address: Department of Bioengineering, Faculty of Engineering, Yokohama National University, Tokiwadai, Hodogaya-ku, Yokohama 240, Japan.
**To whom correspondence should be addressed at: Department of Pure and Applied Sciences, The University of Tokyo, Komaba, Meguro-ku, Tokyo 153, Japan.

tion in mammals. Around 1970, various spectroscopic studies using NMR (Johnson et al., 1969; Urry et al., 1970; Urry and Walter, 1971; Brewster et al., 1973b; Honig et al., 1973; Deslauriers et al., 1974; Walter et al., 1974), laser Raman and circular dichroism techniques (Glickson, 1975; Hruby et al., 1978), were devoted to elucidating the conformation of oxytocin in solution. It was found that oxytocin in aqueous solution is flexible and has an almost random structure, but in dimethyl sulfoxide (DMSO) it assumes a rigid conformation. The local conformation in the β-turn involving the endocyclic residues Tyr-Ile-Gln-Asn, however, is still unclear with respect to the presence of a hydrogen bond between the Asn^5 peptide NH group and the Tyr^2 carbonyl moiety. X-ray structures of deamino-oxytocin (1-mercaptopropionate-oxytocin), which lacks the N-terminal amino group but is more active than the natural hormone (Ferrier et al., 1965), exhibited at least two conformers about the chirality of the disulfide bridge (Wood et al., 1986). The two conformers exhibit a β-turn structure (type II) between Tyr^2 and Asn^5, stabilized by two hydrogen bonds between the amide and carbonyl groups of both residues.

The assignments of almost all of the proton resonances of oxytocin in DMSO have been reported (Johnson et al., 1969; Brewster et al., 1972,1973b). In these assignments, however, some contradiction between authors was apparent in the chemical shifts of the backbone amide protons (Johnson et al., 1969; Walter et al., 1972). Such contradictions also existed in the assignments of the ^{13}C resonances (Brewster et al., 1973a). These contradictions have long been disregarded, though a few researchers have suggested that the variations seen in the assignment of ^1H and ^{13}C resonances in DMSO could arise from the variation in the concentration of hydronium ions in the sample solutions and from an inductive effect of the charge at the N-terminus (Brewster et al., 1973b; Deslauriers et al., 1974). In our spectra, the chemical shifts of the specific protons varied from one sample to another. Distinct variations in the chemical shifts were observed for the Tyr^2 NH, Cys^1 CH^{α}, and CH^{β} resonances.

In order to clarify the cause of the disagreement in chemical shifts, we investigated the proton spectral behavior by varying the solution conditions and we found that the presence of a small amount of base or acid can cause the shift differences described above. All backbone protons and β protons, especially near the N-terminal group, changed their positions in the spectra, depending upon the amount of added base or acid. This acid–base titration experiment may well explain the disagreement in chemical shifts noted in earlier reports. Two spectra of extreme forms were obtained: one of oxytocin with an NH_2 N-terminal amino group at basic pH (hereafter termed 'unprotonated form'), and the other of oxytocin with an $NH_3^+Cl^-$-terminal group at acidic pH (hereafter termed 'protonated form').

We observed small but distinct differences in various NMR parameters, such as chemical shifts and J couplings, between the protonated and the unprotonated forms. All this evidence is, however, indirect and inconclusive because these NMR parameters are often influenced by the inductive effect of protonation at the N-terminus, irrespective of structural changes. Therefore, a direct approach, relying on NMR methods using NOE measurements and distance analysis (Wüthrich, 1986) had to be used. Fortunately, a large number of NOEs were observed in both forms, in spite of the low molecular weight of oxytocin. Thus, using computer calculations based on quantitative NOE analysis, we can expect results with high resolution in this comparative study of the peptide conformation. This kind of study, then, gives an experimental basis for model calculations on the effect of changes in the electrostatic energy upon the local structure in peptides.

This report is divided into two parts. The first part is devoted to establishing the ^1H and ^{13}C

resonance assignments for the protonated and unprotonated forms of oxytocin in DMSO, using a combination of various 2D NMR techniques. NMR parameters relevant to conformation, such as the temperature dependence of the amide proton resonances, ^{1}H and ^{13}C chemical shifts, and three-bond coupling constants (for NH-CH^{α}, CH^{α}-CH^{β} and C'-CH^{β}), were recorded for both forms. We also performed stereospecific assignments of the prochiral β protons, using homonuclear coupling constants for CH^{α}-CH^{β} and heteronuclear coupling constants for C'-CH^{β} (Kessler et al., 1987; Hofmann et al., 1989; Hansen et al., 1991). The second part of this report covers our comprehensive investigation of the oxytocin conformations reflected in the NOEs. The conformational analysis of the protonated and the unprotonated forms was done using distance-analysis calculations (Braun and Gō, 1985; Endo et al., 1991) with NOE constraints derived from a relaxation matrix analysis. The computer program employed is similar to that proposed by Madrid et al. (1991). Whether the observed differences in NMR parameters must be attributed either to the pure inductive effect or to its combination with a conformational change is discussed. A comparison of the calculated structures is made for the tocin ring moiety, including the β-turn structure.

MATERIALS AND METHODS

Sample preparation

Oxytocin was purchased from the Peptide Institute, Inc. (Osaka, Japan) and used without further purification. A hydrochloride salt of oxytocin was used as a control sample of the protonated form of oxytocin. The unprotonated form of oxytocin was prepared as follows. After dissolving the peptide in H_2O, aqueous sodium-acetate solution was added to the sample solution. The amount of sodium acetate to be added was determined by either acid or base titration experiments in DMSO (see the first section in Results): about 0.2 mg of acetate was used for 2 mg of peptide in 0.5 ml of solvent. After lyophilization, the oxytocin was dissolved in deuterated dimethyl sulfoxide (DMSO-d_6, 99.96%). The sample concentration was around 4 mM for ^{1}H NMR analysis and 10 mM for ^{13}C NMR analysis.

NMR analysis

All NMR spectra were recorded on a JEOL GSX400 spectrometer. Tetramethylsilane (TMS) was used as an internal reference for ^{1}H NMR spectra and DMSO (39.5 ppm) for ^{13}C NMR spectra. For both analyses, chemical shifts were finally referenced to TMS. Sequential assignment of the proton resonances was performed utilizing various 2D NMR techniques (Wüthrich, 1986): DQF-COSY (Rance et al., 1983) at 36 °C and NOESY (Jeener et al., 1979; Kumar et al., 1980) at 23 °C and a mixing time of 400 ms. The ^{13}C resonances were assigned from the proton assignments using proton-detected heteronuclear (^{1}H-^{13}C) shift-correlation methods, i.e. HMQC and HMBC (Bax et al., 1983; Bax and Summers, 1986), recorded at 36 °C. Temperature dependent chemical shifts of the amide protons were determined from 1D proton spectra, measured between 20 and 59 °C

Homonuclear coupling constants for NH-CH^{α} (denoted as $^{3}J_{NH\text{-}CH\alpha}$), reflecting the backbone dihedral angles ϕ, were obtained by direct inspection of the resolution-enhanced 1D spectra at 47 °C, where all the amide proton resonances were well resolved. Coupling constants for CH^{α}-CH^{β} (denoted as $^{3}J_{CH^{\alpha}\text{-}CH^{\beta}}$), which provide an estimate of the dihedral angles χ^{1} and stereospecific

assignments of β-methylene protons, were determined by direct analysis of multiplet patterns of P.E. COSY spectra (Müller, 1987). Heteronuclear coupling constants for C'-CH^{β} (denoted as $^3J_{C'\text{-}CH\beta}$) were obtained from proton-detected heteronuclear 2DJ spectra in natural abundance by optimizing the delay time for long-range couplings (Pratum et al., 1988).

The procedure to assign prochiral protons of side chains was as follows. Because the coupling constant $^3J_{CH\alpha\text{-}CH\beta}$ cannot provide sufficient information to fix the prochirality around χ^1, homo- and heteronuclear three-bond coupling constants (i.e., $^3J_{CH\alpha\text{-}CH\beta}$ and $^3J_{C'\text{-}CH\beta}$) were used in combination to complement this information (Kessler et al., 1987; Hofmann et al., 1989; Hansen, 1991). The notation by Wagner et al. (1987) was applied for three rotamers, **1**, **2** and **3**, corresponding to χ^1 values of 60° (g^2g^3), ± 180° (g^2t^3), and −60° (t^2g^3), respectively. To distinguish conformations **2** and **3**, we utilized the rule that for conformation **3** both $^3J_{C'\text{-}CH\beta}$ coupling constants for methylene protons are small, while in conformation **2** one of the coupling constants is small and the other one is large (Kessler et al., 1987). In this way, the CH^{β} and $CH^{\beta'}$ resonances (denoting protons shifted downfield and upfield, respectively) could be distinctively identified as $CH^{\beta 2}$ and $CH^{\beta 3}$ for each amino acid.

Two problems occur in the determination of $^3J_{C'\text{-}CH\beta}$ with the heteronuclear 2DJ technique. First, the coupling constants derived from the 2DJ spectra can only be determined for sharp CH^{β} proton resonances because the multiplets overlap, due to not only the heteronuclear coupling of interest but also a homonuclear coupling. Second, coupling constants are overestimated due to the absolute-value representation of cross peaks (Neuhaus et al., 1985). The coupling constant $^3J_{C'\text{-}CH\beta}$, obtained from the 2DJ spectra, and the relative intensities in HMBC spectra were used to remove the ambiguity in determining the coupling constants for broad resonances. Qualitative estimation of these coupling constants was carried out by comparing the relative intensities of the HMBC cross peaks of the two geminal protons recorded with two delay times, 25 and 50 ms.

The NOESY spectra for the relaxation matrix analysis were recorded at mixing times τ_m = 50, 100, 200, 400, 600 and 800 ms at 23 °C. All of the time-domain data were transformed to give an absorption-phased spectrum of 1024 × 2048 data points. The interval between scans was set at more than 4 or 5 times T_1 to assure spin equilibrium. The NOESY peak intensities were evaluated by volume, using the integration routine of the NMR2/Distance software package together with the JML-S1000 MolSkop system (JEOL). A rectangular box around the peak of interest was used for all integrals. In this curve-fitting routine, the integrals of peaks with sharp spectral line shapes are overestimated, and those of broader peaks are underestimated, because each peak is fitted with a single Gaussian curve for both the ω_1 and ω_2 dimensions. The value of a cross-peak volume, V, was corrected by referring to the volumes for the two diagonal peaks, corresponding to two protons, producing the cross peak as follows (Eq. 1):

$$V_{corrected} = V\frac{\sqrt{I_1 \cdot I_2}}{I_0} \tag{1}$$

Here, I_1 and I_2 are the volumes of two diagonal peaks and I_0 is the mean diagonal peak volume that reflects one spin intensity. The most influential factor limiting the quantitative analysis of NOESY spectra is the peak overlap. The volumes of all overlapped peaks were positively taken into account in the computer analysis for the relaxation matrix, by evaluating them as the sum of intensities of overlapped peaks.

Relaxation matrix determined from NOE intensities

The relaxation matrix was obtained by fitting the calculated spectra to the experimental ones for all mixing times. The 2D NOESY spectra were simulated according to Eq. 2 (Macura and Ernst, 1980):

$$M(\tau_m) = e^{-\mathbf{R}\tau_m} M(0) \tag{2}$$

Here, **R** is the relaxation matrix, in which the diagonal elements correspond to the spin-lattice relaxation rates and $M(\tau_m)$ represents the signal intensities in the 2D NOESY spectra. The difference between the calculated and experimental spectra was minimized by varying the relaxation matrix according to a nonlinear least-squares method (Levenberg–Marquadt algorithm). The initial matrix **R** was estimated by applying Eq. 3 to the signal intensity $M(\tau_m)$ at τ_m = 200 ms.

$$\mathbf{R} = \frac{-\ln\left(\frac{M(\tau_m)}{M(0)}\right)}{\tau_m} \tag{3}$$

The initial magnetization, M(0), was estimated by using the peak intensities of diagonal peaks at τ_m = 0.005 ms as a reference point. The peak intensities of overlapped signals (e.g., diagonal signals) were not used in the iterative fitting. The computer program we used is similar to that proposed by Madrid et al. (1991).

Interpretation of the relaxation matrix

The obtained relaxation matrix was analyzed by assuming that the NOEs were derived from a single conformation. In a rigid structure, the NOEs between two protons separated by a fixed distance r_0, such as methylene protons, are used to calibrate other NOEs (r_0 = 1.75 Å). The distance to be measured, r_{ij}, is then given by $Q(r_{ij}) = \sigma_{ij}/\sigma_0 = (r_0/r_{ij})^6$, in which σ_{ij} is the cross-relaxation rate for spins i and j, and σ_0 is that measured for the known distance r_0. This rigid model is, however, inappropriate when applied to oxytocin, because of the inherent flexibility of the peptide structure. To adapt the relaxation matrix analysis to the well-known structure-determination procedure with distance analysis (Wüthrich, 1986), which uses the internuclear distances as lower and upper bounds, a model to interpret the matrix in this framework is required.

To account for the flexibility of the molecular structure, Braun et al. (1981) introduced a dynamical model in which the distance between proton spins i and j is allowed to vary uniformly between a minimum r_m and a maximum R_m (uniform averaging model). This leads to an effective cross-relaxation rate, σ_{ij}^e, given by Eq. 4:

$$\sigma_{ij}^e = \left\langle \frac{f(\tau_{ij})}{r^6} \right\rangle = \frac{f(\tau_{ij})}{5(R_m - r_m)} \left(\frac{1}{r_m^5} - \frac{1}{R_m^5} \right) \tag{4}$$

Here, $f(\tau_{ij})$ is a function of the correlation time τ_{ij} for the dipole–dipole interactions between spins i and j. $Q(R_m)$ is defined to obtain a quantity that can readily be compared with $Q(r_{ij})$, as expressed by Eq. 5:

$$Q(R_m) \equiv \frac{r_0^6}{5(R_m - r_m)} \left(\frac{1}{r_m^5} - \frac{1}{R_m^5} \right) \tag{5a}$$

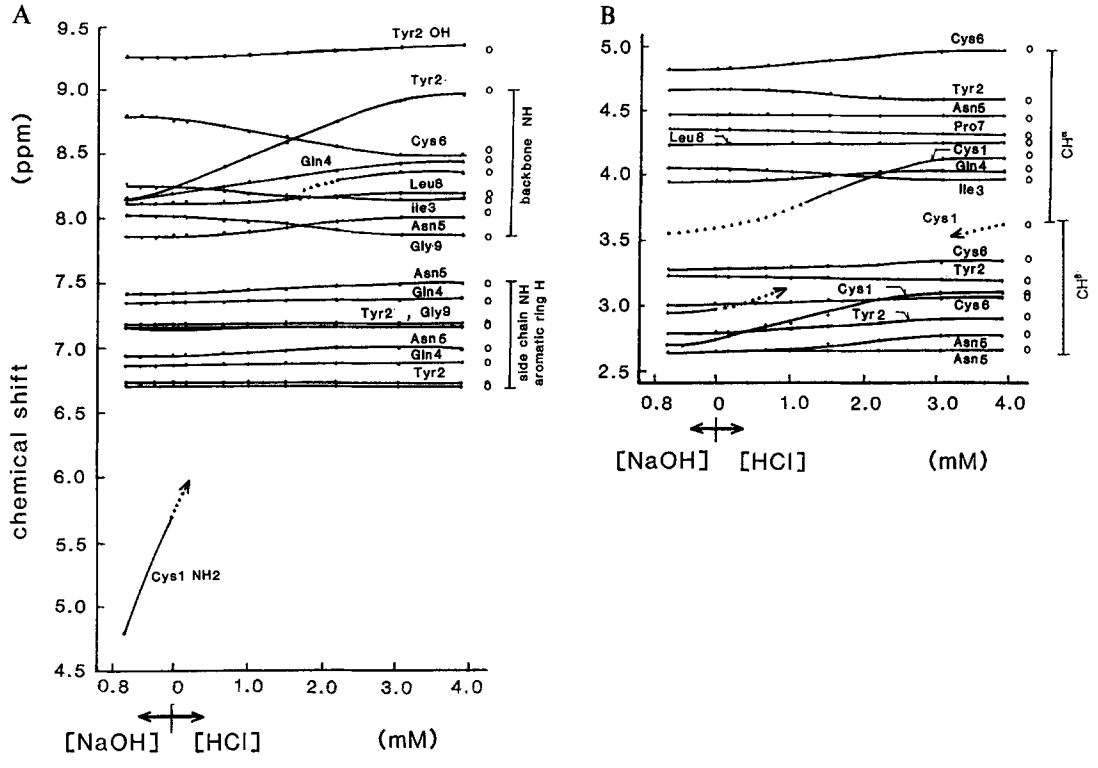

Fig. 1. Chemical-shift changes in (A) the lower field region and (B) the higher field region plotted as a function of hydroxide or hydronium ion concentration during acid–base titration of oxytocin in DMSO at 23 °C. Sample concentration was 3.7 mM, and the 'o' marks show the values for oxytocin hydrochloride. Dotted lines denote chemical shifts in the region where the water peak overlapped.

$$\geq \frac{f(\tau_{ij})}{f(\tau_R)} \frac{r_0^6}{5(R_m - r_m)} \left(\frac{1}{r_m^5} - \frac{1}{R_m^5}\right) = \frac{\sigma_{ij}^e}{\sigma_0} \tag{5b}$$

Here, τ_R is an overall rotational correlation time. In Eqs. 4 and 5, r_m was set at 2.0 Å, the van der Waals contact distance between two protons, because r_m cannot presently be determined empirically (Braun et al., 1981).

We utilized this approach to adapt the relaxation matrix to the established distance analysis, and thus interpret this analysis in terms of upper and lower limits of the distances. To do so, the assumption of the lowest possible limit for r_m was found to be impractical, because a value of Q smaller than 0.05 leads to a very large value ($\gg$ 10.0 Å) of R_m. We then modified the uniform averaging model to vary r_m in proportion to R_m, defining a rigidity parameter, x, as $x = r_m/R_m$. Using this model, all the cross-relaxation rate elements were successfully converted to the upper bounds of interproton distances, as follows:

$$R_m = r_0 \left\{ \frac{\sigma_0}{\sigma_{ij}} \cdot \frac{1 - x^5}{5x^5(1 - x)} \right\}^{1/6} \tag{6}$$

$$r_m = x \cdot R_m \tag{7}$$

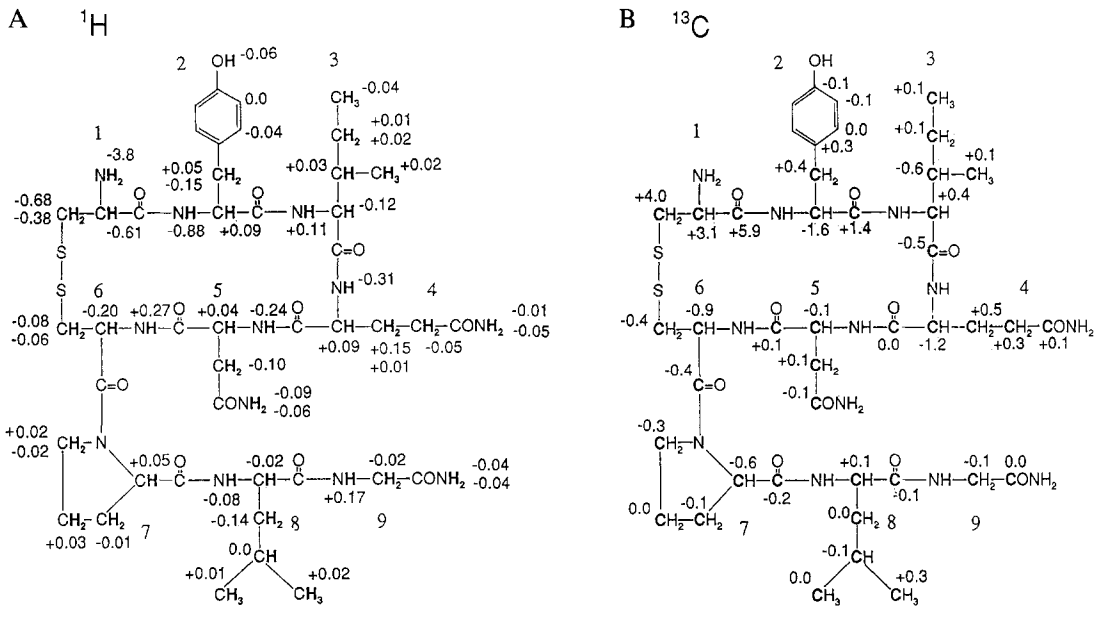

Fig. 2. Chemical-shift changes of ^{1}H nuclei (A) and ^{13}C nuclei (B) of oxytocin upon deprotonation of the N-terminal amino group in DMSO. Plus and minus signs indicate downfield and upfield shifts (in ppm), respectively.

Distance analysis calculation

Distance analysis calculations were performed by using a set of upper limits on the interproton distances obtained from Eqs. 6 and 7, by varying the rigidity parameter x from 0.9 to 0.5. We used the DADAS90 program (Endo et al., 1991) of the JML-S1000 MolSkop system (JEOL). This program is an extended version of DADAS (Distance Analysis in Dihedral Angle Space, sometimes called DISMAN) (Braun and Gō, 1985) that minimizes a variable target function with the rapid second-derivative calculation and generates an unbiased structure (Endo et al., 1991). Starting from random structures, a set of 200 folded structures was generated for each rigidity parameter for the two forms of oxytocin. In our study, the ω angles were fixed at 180°. All calculations were performed on a Titan 3000 computer (Kubota Computer Inc.).

RESULTS

Assignment of ^{1}H resonances for the protonated and unprotonated forms of oxytocin

We quantitatively studied the influence of acid and base on the spectral behavior of oxytocin in DMSO. Concentrated aqueous hydrochloric acid and sodium hydroxide (or sodium acetate) solutions were used for the titrations; shifts in the resonance frequencies and changes in the line shapes of all protons were followed by progressively adding either base or acid to the sample solutions. Chemical-shift variations of individual proton resonances were plotted as a function of concentration of the added base or acid, as shown in Fig. 1. Each of the proton resonances exhibited a single sigmoidal titration curve. The large downfield shift in the N-terminal amino and Tyr^{2} backbone NH protons (Fig. 1A), and Cys^{1} CH^{α} and CH^{β} protons (Fig. 1B) is therefore interpreted in terms of two chemically different states, associated with the protonation of the

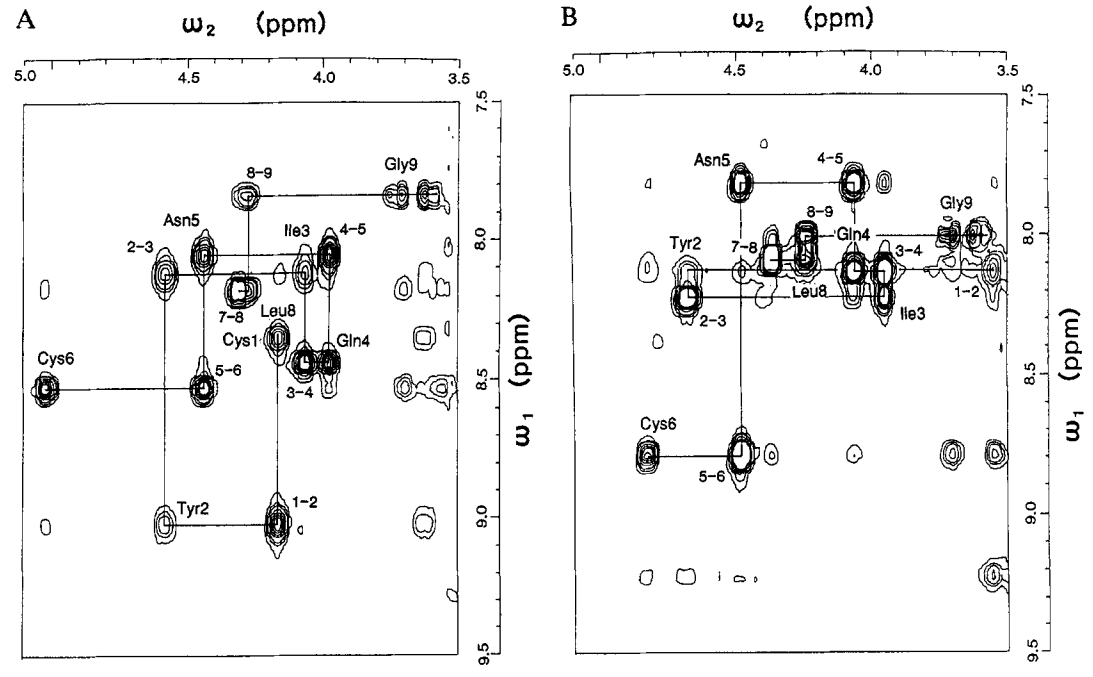

Fig. 3. Fingerprint regions of 400 MHz NOESY spectra for the two forms of oxytocin, protonated (A) and unprotonated (B), with a mixing time of 400 ms (5.0 mM at 23 °C). Specific sequential resonance assignments are shown. The spectra were recorded with 1024 points in ω_2 and 512 points (zero-filled from 256 points) in ω_1 over a spectral width of 4200 Hz.

N-terminal amino group. One is oxytocin in the basic state, with an NH_2-terminal group (i.e., unprotonated form), and the other is oxytocin in the acidic state with an $NH_3^+Cl^-$-terminal group (i.e., protonated form). A plateau of each shift variation in the acidic state agrees well with that of oxytocin hydrochloride. Almost all of the backbone proton resonances of both the cyclic and acyclic parts of the peptide were affected upon protonation. The maximum changes in the chemical shifts of individual protons of oxytocin during the titration are shown in Fig. 2A.

We also investigated the effect of water contamination and recorded the proton spectral change of oxytocin when a small amount of water was added to the sample solutions. This water-titration experiment resulted in little change in both chemical shift and line shape of individual proton resonances, up to about 2% water content. In the course of the acid–base titration, the water content was increased only to about 1.5%, thus we conclude that the presence of water is not responsible for the observed spectral changes.

Using the established procedure of sequential resonance assignment (Wüthrich, 1986), all of the proton resonances were unambiguously assigned for protonated and unprotonated oxytocin in DMSO. The sequential connectivity of each of the two forms of oxytocin is shown in Fig. 3 (note that for the Cys^6–Pro^7 connectivity, the cross peak between Cys^6 CH^α and Pro^7 CH^δ was used). Aromatic ring protons of Tyr^2 were connected to CH^β protons with the aid of the NOESY spectrum. Based on the results from NOE data, the side-chain amide protons of Gln^4 and Asn^5, and the C-terminal amide protons of Gly^9 were also connected, to the CH^γ, CH^β and CH^α protons of each residue, respectively. The peak assignments of the protons of each residue are illustrated for the two forms in Fig. 4.

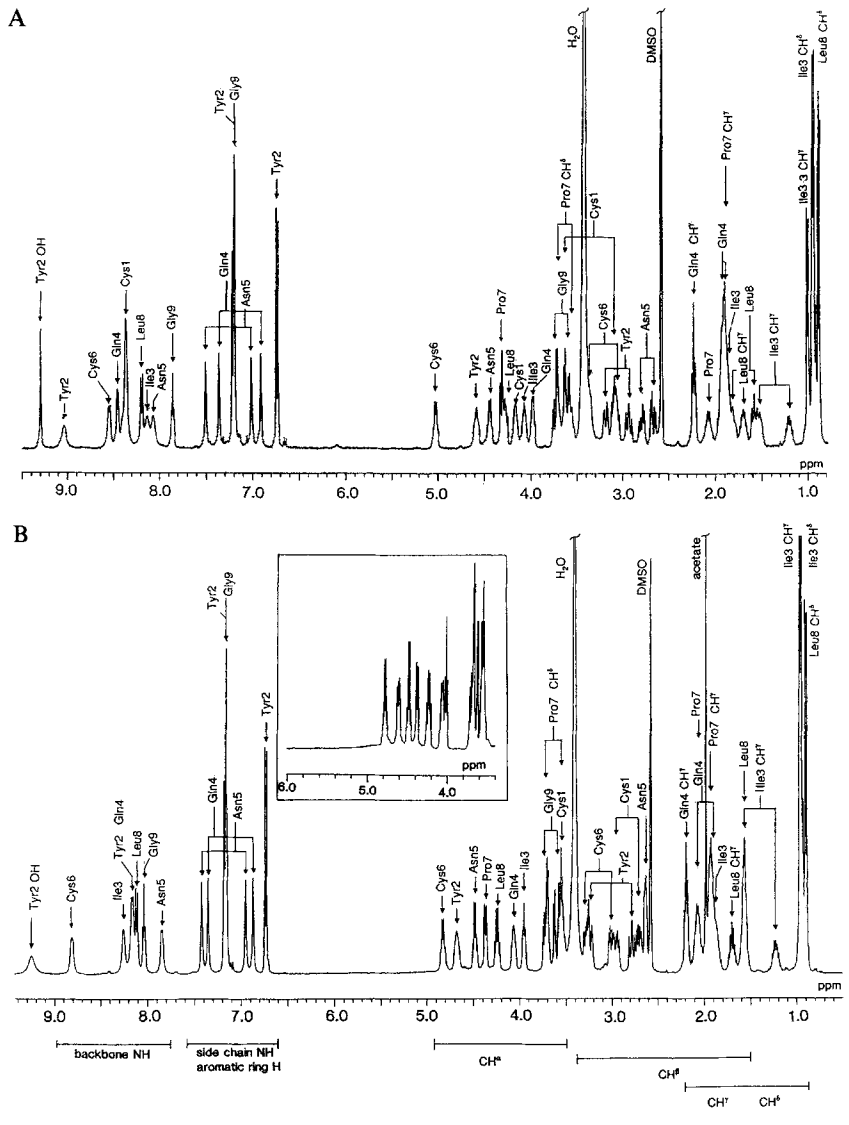

Fig. 4. 400 MHz proton NMR spectra for the N-terminal protonated (A) and unprotonated (B) forms of oxytocin in DMSO (5.0 mM at 23 °C), showing the ^{1}H spectral assignment. The inset in (B) shows a broad N-terminal amino resonance in the unprotonated form overlapping with the α proton resonances at 59 °C.

In previous reports, the N-terminal amino proton resonance was not identified (Glickson et al., 1972); In Fig. 4A, however, it is clearly identifiable in the protonated form at 8.36 ppm. This resonance is severely broadened in the unprotonated oxytocin, explaining the difficulty of recognizing the peak in previous work. We have two pieces of evidence for this assignment: a cross peak to Cys^1 CH$^\alpha$ in the DQF-COSY, and the intensity of three protons estimated in the 1D spectrum. Contrary to this observation, in Fig. 4A this resonance in the unprotonated form was not found at room temperature, but it did appear as a very broad resonance around 4.6 ppm when the

temperature was raised to 59 °C (shown in the insertion in Fig. 4B). The acid–base titration curves were also consistent with the assignments of the two forms.

Assignment of ^{13}C resonances for the protonated and unprotonated forms of oxytocin

Using proton-detected heteronuclear correlation spectroscopy (i.e., a combination of HMQC and HMBC techniques) all of the ^{13}C resonances were unambiguously assigned from the known proton resonance assignments. The ^{13}C resonances of proton-attached nuclei were straightforwardly identified in the HMQC spectra. The assignment of the carbonyl carbons (C') was done using HMBC spectra, optimized for long-range couplings, in which C' regions were selectively excited to enhance sensitivity in the spectra. Correlations between the C' and aliphatic protons are shown in Fig. 5. The long-range couplings of backbone carbonyl carbons to CH^{α} protons of the adjacent residue (i.e., $^{3}J_{C'(i)\text{-}CH^{\alpha}(i+1)}$) are useful in tracing out sequential connectivities of the backbone amino acids. Thus, we could identify all the backbone carbonyl carbons; the couplings of Tyr^2 CH^{α} to both adjacent carbonyl carbons (Tyr^2 C' and Cys^1 C') and the coupling of Pro^7 CH^{α} to Cys^6 C' were missing, probably due to the short T_2 times of these protons. The correlation between intraresidue C' and CH^{β}, or C' and NH atoms was used to complement the other evidence. Side-chain carbonyl carbons, Gln^4 C^{δ} and Asn^5 C^{γ}, were assigned with the aid of cross peaks to Gln^4 CH^{α} and Asn^5 CH^{γ}, respectively.

Another piece of information obtained from carbon resonances is the chemical shift of the γ carbon of proline (which correlates with either the cis or trans conformation of the preceding peptide bond) (Deslauriers et al., 1972; Thomas and Williams, 1972; Wüthrich et al., 1972; Brewster et al., 1973a; Dorman and Bovey, 1973). Both the protonated and unprotonated forms of oxytocin showed the typical γ carbon chemical shifts for the trans Cys^6-Pro^7 bond. The maximum changes in chemical shift for each individual ^{13}C of oxytocin in the titration are shown in Fig. 2B.

Stereospecific assignments of side-chain protons

Table 1 shows the results of the stereospecific assignment of the β-methylene protons obtained by combining homo- and heteronuclear three-bond coupling constants (i.e., $^{3}J_{CH^{\alpha}\text{-}CH^{\beta}}$ and $^{3}J_{C'\text{-}CH^{\beta}}$) with qualitative NOE data. In the protonated form, the β protons for five residues (i.e., Cys^1, Tyr^2, Asn^5, Cys^6 and Leu^8) were stereospecifically assigned. One of the two CH^{β} protons in the Asn^5 and Cys^6 residues exhibited a relatively strong cross peak to each carbonyl carbon in the HMBC spectrum (Fig. 5A) and was assigned to $CH^{\beta 2}$ in rotamer **2** and to $CH^{\beta 3}$ in rotamer **1**. We used qualitative NOE data, since $^{3}J_{CH^{\alpha}\text{-}CH^{\beta}}$ values, in the intermediate range (5–9 Hz), were not decisive in distinguishing rotamers. Because strong NOE(α,β) peaks were observed for Asn^5, the CH^{β} proton that exhibited a stronger cross peak to the carbonyl carbon in the HMBC spectrum was assigned to $CH^{\beta 3}$ in rotamer **1** (Fig. 5A). On the other hand, as strong NOE(NH,β) peaks were observed in Cys^6, the CH^{β} proton that exhibited a stronger cross peak to the carbonyl carbon in the HMBC spectrum was assigned to $CH^{\beta 2}$ in rotamer **2**. Both CH^{β} protons of Cys^1, Tyr^2 and Leu^8 had weak cross peaks to carbonyl carbons in the HMBC spectrum and the CH^{β} proton with the largest coupling to the CH^{α} proton is to be assigned to $CH^{\beta 2}$. In the unprotonated form, CH^{β} protons for four residues (i.e., Cys^1, Tyr^2, Gln^4 and Cys^6) were assigned in the same way (Fig. 5B). If $^{3}J_{CH^{\alpha}\text{-}CH^{\beta}}$ has an intermediate value (5–10 Hz), the skewed rotamers (Hansen, 1991) should also be considered. In the protonated form, the CH^{β} protons of Asn^5 and Cys^6 were

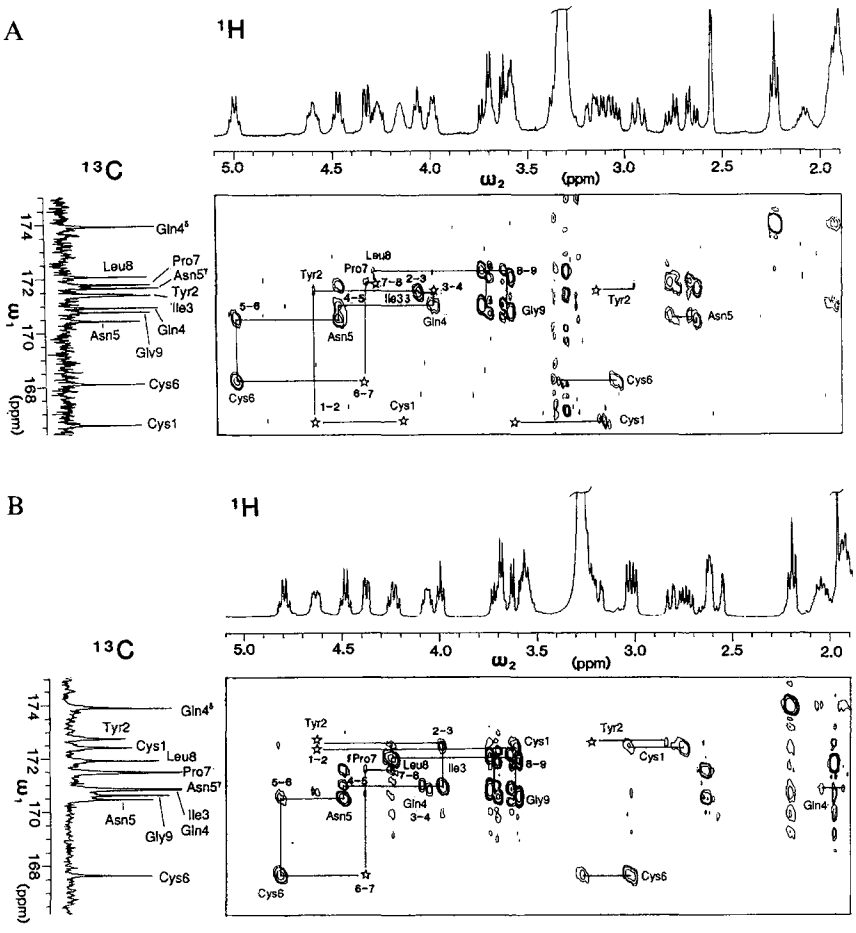

Fig. 5. 400 MHz HMBC spectra for the protonated (A) and unprotonated (B) forms of oxytocin at 36 °C, showing the C'-CH$^\alpha$ and C'-CH$^\beta$ regions. Solution concentrations were 5.0 mM for the protonated and 20.0 mM for the unprotonated form. Sequential connectivities (C'_i–CH^α_{i+1}) and the assignments of carbonyl carbons are shown. Connections for two prochiral β protons are marked by horizontal bars, and very weak or missing connected peaks are marked by a ☆. The delay time was 50 ms, optimized for long-range couplings. The spectra were recorded with 1024 points in ω_2 and 512 points (zero-filled from 64 points) in ω_1. Spectral widths were 4200 Hz in ω_2 and 2000 Hz in ω_1, and the C'O region in the ω_1 direction was selectively excited to reduce the spectral width.

probably skewed from rotamers **1** and **2**, respectively, and in the unprotonated form, those of Cys^1 and Cys^6 were also skewed from rotamers **3** and **2**, respectively. The γ methylene protons of Ile^3 were assigned by using only qualitative NOE intensities of (CH^β,CH^γ), (CH^β,$CH^{\gamma'}$), (CH_3^γ,CH^γ) and (CH_3^γ,$CH^{\gamma'}$) interactions. The low-field CH^γ proton was assigned to $CH^{\gamma 3}$ in the protonated form and to $CH^{\gamma 2}$ in the unprotonated form.

NMR parameters relevant to the solution conformations

It is well known that the electron-withdrawing side chains generally accelerate the exchange rate of neighboring peptide protons, and move their resonance frequencies downfield (Sheinblatt, 1966; Molday et al., 1972). The N-terminal amino protons and protons nearby exhibited remark-

TABLE 1
SUMMARY OF STEREOSPECIFIC ASSIGNMENTS OF β-METHYLENE PROTONS FOR THE PROTONATED AND UNPROTONATED FORMS OF OXYTOCIN

Residue	NOE connectivities				$^3J(\alpha,\beta)$[a] (Hz)	$^3J(\alpha,\beta')$[a] (Hz)	$^3J(C'O,\beta)$[b] (Hz)		$^3J(C'O,\beta')$[b] (Hz)		Assignment[c]		χ^1[f] (°)
	(NH,β)	(NH,β')	(α,β)	(α,β')							β	β'	
Protonated													
Cys^1	w	m	s	s	4.7	8.0	–[d]	(–)[e]	m	(10)[e]	β3	β2 (**3**)	−87, +49
Tyr^2	w	m	s	m	3.7	10.4	–	(–)	w	(–)	β3	β2 (**3**)	−92
Asn^5	w	w	s	s	7.3	6.3	m	(9)	s	(10)	β2	β3 (**1**)	−126, +43
Cys^6	m	s	s	s	6.0	7.3	w	(–)	s	(8)	β3	β2 (**2**)	±163
Leu^8	s	m	w	m	10.5	4.9	–	(–)	–	(–)	β2	β3 (**3**)	
Unprotonated													
Cys^1	–	–	s	s	6.6	7.3	w	(< 9)	m	(10)	β3	β2 (**3**)	−116
Tyr^2	m	m	s	m	4.7	10.7	–	(6)	w	(6)	β3	β2 (**3**)	−119
Gln^4	m	m	s	s	4.4	9.1	w	(–)	w	(–)	β3	β2 (**3**)	−86
Cys^6	m	s	m	s	6.9	7.3	w	(6)	s	(9)	β3	β2 (**2**)	+178

[a] Coupling constants were determined directly from the multiplet patterns of cross peaks in the P.E.COSY spectra.
[b] Coupling constants were determined from HMBC and ^{1}H-detected 2DJ spectra.
[c] β is the lowfield β proton and β' is the highfield β proton. The rotamer types **1**, **2** and **3** are shown in parentheses.
[d] Values were undetectable or missing.
[e] Values in parentheses are apparent coupling constants, obtained from projection spectra in ω_2 of ^{1}H-detected 2DJ spectra, in which doublet splittings correspond to the coupling constants.
[f] Calculated χ^1 angles with the lowest target function using distance analysis. Two χ^1 angles were obtained for the Cys^1, Asn^5 and Cys^6 residues in the protonated form. w is weak, m is medium and s is strong.

able chemical-shift changes, mainly due to the inductive effect of protonation at the N-terminus (0.1–1.0 ppm). Similar to the changes in the ^{1}H resonances, large changes in the ^{13}C chemical shifts were observed for carbons near the N-terminus (1–6 ppm), as shown in Fig. 2B. In addition to these changes, changes were also observed in the resonances of aliphatic protons, aliphatic carbons and carbonyl carbons, even at eight bonds or more from the N-terminus.

The temperature coefficients, $-\Delta\delta/\Delta T$, for peptide amide proton resonances, which offer information about contributions of amide protons to hydrogen bonds, were obtained from the shift variations occurring when the temperature was increased from 20 to 59 °C (Table 2). In the protonated form, all NH proton resonances were temperature dependent, with temperature coefficients ranging from 2 to 7 ppb/°C. On the other hand, in the unprotonated form, no temperature dependence (i.e., temperature coefficients of 0 ppb/°C) was observed for Tyr[2] NH and Asn[5] NH, suggesting that these protons either take part in intramolecular hydrogen bonds or are not exposed to the solvent. The coefficients for Ile[3], Gln[4], Cys[6], Leu[8] and Gly[9] ranged from 5 to 10 ppb/°C. The values of coupling constant $^{3}J_{NH\text{-}CH\alpha}$, which provide an estimation of the backbone torsion angle ϕ, are summarized in Table 2. The Tyr[2] NH resonance in the unprotonated form was too broad to allow determination of the coupling constant. Differences between the two

TABLE 2
PROPERTIES OF AMIDE PROTONS FOR THE PROTONATED AND UNPROTONATED FORMS OF OXYTOCIN

Residue	NH (ppm)	$-\Delta\delta/\Delta T$[a] (ppb/°C)	$^{3}J(NH,\alpha)$[b] (Hz)	ϕ_{exp}[d] (°)	ϕ_{cal}[e] (°)
Protonated					
Tyr[2]	9.03	1.7	8.2	<u>−147</u>, −93	−157 ± 11
Ile[3]	8.14	4.5	5.9	−167, <u>−74</u>, +35, +85	−95 ± 4
Gln[4]	8.46	4.2	4.4	<u>−178</u>, −62, +18, +102	+168 ± 7
Asn[5]	8.07	4.0	7.0	<u>−158</u>, −82, +60	−175 ± 2
Cys[6]	8.54	6.1	7.7	<u>−152</u>, −88	−135 ± 5
Leu[8]	8.19	4.7	7.9		
Gly[9]	7.86	3.2	5.9		
Unprotonated					
Tyr[2]	8.15	0.0	–[c]	–	−107 ± 5
Ile[3]	8.25	8.9	6.4	−162, <u>−78</u>, +43, +75	−91 ± 1
Gln[4]	8.15	4.3	6.4	<u>−162</u>, −78, +43, +75	−166 ± 7
Asn[5]	7.83	0.0	6.5	<u>−162</u>, −78, +43, +75	+177 ± 2
Cys[6]	8.81	10.4	7.9	<u>−150</u>, −90	−136 ± 1
Leu[8]	8.11	6.3	7.6		
Gly[9]	8.03	5.5	5.9		

[a] Temperature coefficient observed for the range from 20 to 59 °C.
[b] Values were determined from 1D spectra at 47 °C.
[c] Tyr[2] NH resonance was too broad to allow determination of the coupling constant.
[d] ϕ angles obtained from $^{3}J_{NH\text{-}CH\alpha}$ coupling constants in the cyclic moiety. ϕ angles which agree well with those for calculated structures (ϕ_{cal}) are underlined.
[e] ϕ angles of calculated structures with the lowest target-function values.

forms of oxytocin in $^3J_{NH\text{-}CH^\alpha}$ for residues in the cyclic moiety were larger than those in the acyclic part (i.e., 0.2–2.0 Hz), suggesting conformational differences in the backbone of the cyclic moiety.

Determination of the relaxation matrix

In the determination of the relaxation matrix, the calculated cross-peak intensities agreed with the experimental intensities with an accuracy of ± 5–15%, though the peak intensities of overlapped signals (e.g., diagonal signals) were not used in the iterative fitting. With this procedure, the peak intensities at different mixing times, even for the spin-diffusion regime (τ_m = 50 to 800 ms), were reproduced well by a single relaxation matrix. The peaks that showed evidence of exchange with residual water, for example the tyrosine OH resonance, were also included in the calculation.

Distance analysis calculation for the two forms of oxytocin

For both forms of oxytocin, six sets of interproton distances for different rigidity parameters, x, were obtained (x = 0.50, 0.60, 0.65, 0.70, 0.80 and 0.90). A total of 93 interproton distances were used for the protonated form, and 105 for the unprotonated form. For each set of interproton distances, 200 structures were generated. As the distance uncertainty increased, i.e. x decreased, the normalized target function values decreased as expected. These results gave the criteria used in determining appropriate x values at which violations between calculated and experimental distances could be minimized: x = 0.70 for the protonated form, and x = 0.65 for the unprotonated form. The criteria used in choosing these values for the distance uncertainty for 10 structures that had the lowest target function values were as follows:

(a) The average sum of the distance violations was small (< 1.0 Å);

(b) The average sum of the deviations from the standard distances for a disulfide bridge was within 0.01 Å (note that the distance for Cys^1 S–Cys^6 S was 2.04 Å, and the distances for both Cys^1 C$^\beta$–Cys^6 S and Cys^1 S–Cys^6 C$^\beta$ were 3.05 Å); and

(c) R_m between the CH$^\alpha$ and CH$^\beta$ protons, or between the CH$^\alpha$ and NH protons did not significantly exceed the geometrical upper limits of 2.9 and 2.8 Å, respectively (Wüthrich, 1986).

The results of the distance analysis calculations for the two forms are summarized in Table 3. Of the 200 calculated conformations, 10 structures with the lowest target-function values were selected for each of the two forms. The mean pairwise root-mean-square deviation (r.m.s.d.) values for backbone atoms in the cyclic moiety among 45 pairs of structures with the lowest target

TABLE 3
STRUCTURAL STATISTICS FOR THE PROTONATED AND UNPROTONATED FORMS OF OXYTOCIN

Form	Distance constraints	Target function[a]	No. of violations (> 0.1 Å)[b]	Sum of violations (Å)	r.m.s.d.[c] (Å)
Protonated	93	0.12	0	0.16	0.24 ± 0.13
Unprotonated	105	0.01	0	0.02	0.10 ± 0.08

[a] Values are the average for the 10 conformations with the lowest target function of the protonated and unprotonated forms.

[b] Number of constraint violations that exceed the upper bounds by more than 0.1 Å.

[c] Mean pairwise root-mean-square deviation of backbone atoms N, C$^\alpha$ and C', in the cyclic part among 45 pairs of structures.

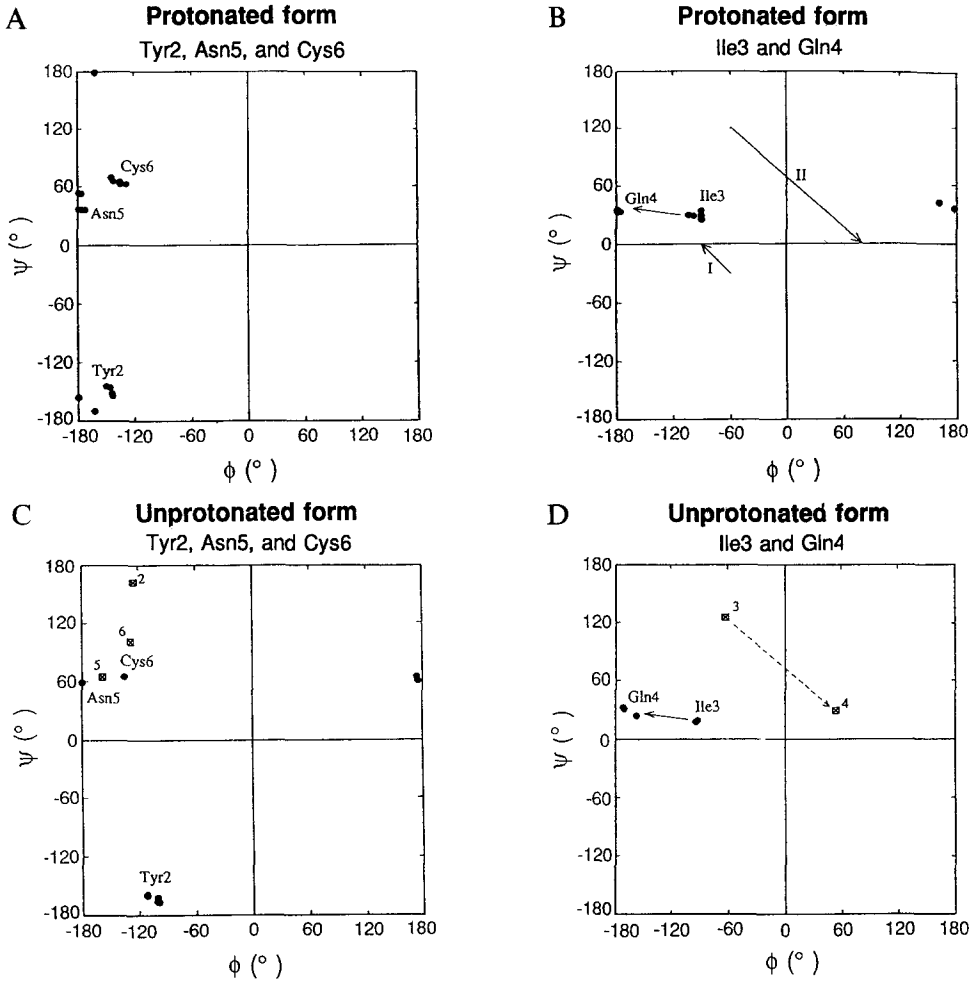

Fig. 6. Ramachandran plots, representative of the dihedral angles of the cyclic moiety for conformations with the lowest target functions, derived from distance analysis calculations. (●) indicates dihedral angles for Tyr^2, Asn^5 and Cys^6 (A and C) and for Ile^3 and Gln^4 (B and D), plotted over 10 conformations for the protonated and unprotonated forms. Ramachandran plots of typical β-turns (type I and II turns) are indicated in B. The mark ⊠ shows the ϕ and ψ angles for the X-ray structures of deaminooxytocin.

function values were 0.24 ± 0.13 Å for the protonated form and 0.10 ± 0.08 Å for the unprotonated form. The mean pairwise r.m.s.d. between the two forms from the 100 (10 × 10) pairs was 0.46 ± 0.06 Å.

Of the interresidue distances for the cyclic moiety, 43 for the unprotonated form and 25 for the protonated form, 15 distances appeared in both forms at the same proton pairs. Among these, the distances that were significantly different between the two forms were those for Tyr^2 NH–Cys^1 $CH^{\beta 2}$, Cys^6 CH^{α}–Tyr^2 NH, Gln^4 NH–Ile^3 NH, Cys^6 NH–Gln^4 CH^{α} and Cys^6 NH–Asn^5 NH. In addition to these 15 common distances, 28 additional distances were found only in the unprotonated form and 10 only in the protonated form. The extra NOEs were all weak and corresponded to distances larger than 3.8 Å.

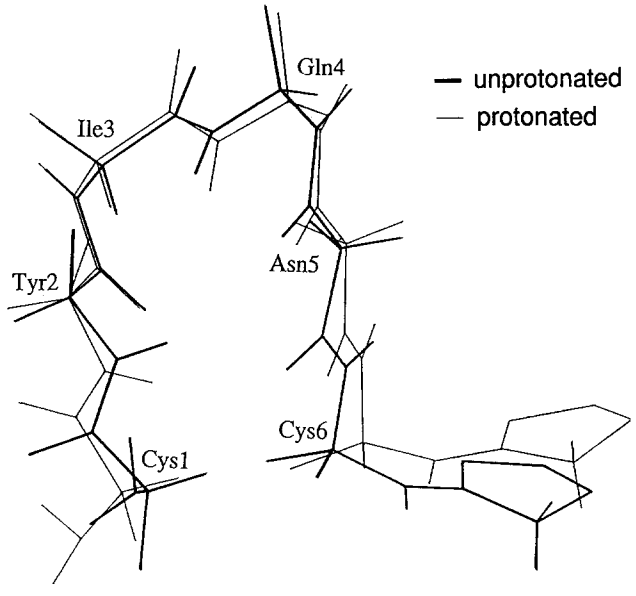

Fig. 7. Superpositions of two conformations, obtained by taking an average over 10 structures that had the lowest target-function value for the protonated and unprotonated forms of oxytocin. The C', C^{α} and N backbone for the cyclic part (Cys-Tyr-Ile-Gln-Asn-Cys) is shown.

exposed to the solvent. The main conformation with the lowest target-function values had no hydrogen bonds in the ring part. Another conformation that had a type-II β-turn structure between Tyr^2 and Asn^5, stabilized by two hydrogen bonds between amides and carbonyls of both the residues, was obtained in the conformation group that had the second lowest target-function values. On the other hand, in the protonated form, the shifts of all NH protons were temperature dependent, which is consistent with an absence of hydrogen bonds, even in the structures of minor conformation groups that had low target-function values.

For Gln^4, there is a significant difference of 2.0 Hz in $^3J_{NH\text{-}CH^{\alpha}}$ and of 1.2 ppm in the chemical shift of α carbons between the two forms (see Table 2 and Fig. 2B). These experimental results agreed well with the somewhat large difference of 26 ± 7° in the φ angle of Gln^4. Local distortion of the S-S dihedral angle must affect not only the backbone conformation of the residues near the ring closure, but also the entire backbone structure in the cyclic part. To confirm the difference in the entire backbone conformation in the cyclic part between the two forms, two results are shown. First, the pairwise r.m.s.d. between the two forms was slightly larger (0.46 ± 0.06 Å) than that for each form (0.24 ± 0.13 Å for the protonated and 0.10 ± 0.08 Å for the unprotonated form). Second, the principal value analysis shown in Fig. 8, which is very informative to compare different conformations in general (Nakai et al., 1993), showed two clusters of conformations; one is compact, corresponding to the unprotonated form, and the other is dispersed, corresponding to the protonated form. These results indicate two things: (i) the backbone conformations of the two forms are well separated, confirming the conclusion mentioned previously regarding the differences in structure; and (ii) the dispersed principal values observed for the protonated form reflect conformers of oxytocin compatible with the finding of the averaged χ^{ss} angle.

Comparisons with backbone dihedral angles from X-ray structures of deaminooxytocin are

In the established method for the determination of structures by using distance calculations (Wüthrich, 1986), the internuclear distances are used as upper and lower bounds, which are subsequently used as input for structural calculations. The NOEs are qualitatively classified as weak, medium or strong, and the corresponding upper distance constraints are calibrated relative to the standard distances. We adapted our relaxation matrix analysis to the established approach to obtain semiquantitative interproton distances, by using a uniform averaging model in which a rigidity parameter x was introduced. This approach should be the most successful way to analyze the NOE data. The rigidity parameter does not necessarily correspond to the actual flexibility of the structure, but rather reflects the redundancy, appearing as the uncertainty in internuclear distance, inherent in the flexible peptide conformation. This mathematical approach is compatible with the flexible nature of the peptide conformation, as evidenced by the many reports of successful structure determinations of proteins in solution by NMR (Hendrickson and Wüthrich, 1992). We applied the same value of x to all protons, which can be interpreted as uncertainty by taking the flexibility of side chains into account, though different rigidity values for backbone and side chains could also be considered (Güntert et al., 1991).

Comparing the calculated conformations with the lowest target function value between the two forms, no significant differences are present between the overall structures, as shown in Fig. 6. The general definition of a β-turn is that the distance between C^{α}_{i} and C^{α}_{i+3} is less than 7 Å, and the residues involved are not helical (Lewis et al., 1973). Variations in β-turn geometries, including classic types of β-turns and their distortions found in proteins, have been described (Wilmot and Thornton, 1990). In both forms of oxytocin, β-turn conformations consisting of the Tyr^2–Asn^5 moiety could not be characterized as any of the proposed β-turns (Figs. 6B and D).

Looking closely at the two structures of the protonated and unprotonated forms of oxytocin, however, local differences can be recognized: five transannular backbone distances between the Tyr^2 and Asn^5 residues, as well as between the Cys^1 and Cys^6 residues (i.e., mean distances for Tyr^2 C'–Asn^5 N, Tyr^2 C^{α}–Asn^5 C^{α}, Tyr^2 N–Asn^5 C', Cys^1 C'–Cys^6 N and Cys^1 C^{α}–Cys^6 C^{α}). In the protonated peptide, these distances were 4.2 ± 0.3, 5.1 ± 0.1, 4.2 ± 0.2, 5.3 ± 0.3 and 4.5 ± 0.4 Å, respectively, whereas in the unprotonated peptide they were shorter, i.e. 4.0 ± 0.1, 4.9 ± 0.1, 3.7 ± 0.2, 4.7 ± 0.1 and 3.9 ± 0.1 Å, respectively. Thus, the protonated form is slightly expanded at the position near the S-S ring closure in the cyclic part (Fig. 7), explaining the difference in backbone dihedral angles for residues near the S-S ring closure (i.e., χ^{ss}, Cys^1 ψ and Tyr^2 ϕ). As for the ring closure, when only the Cys^6 CH^{α} proton shows a NOE connection with the Cys^1 CH^{α} and Cys^1 CH^{β} protons, and Cys^1 CH^{α} does not show any connection with the Cys^6 CH^{β} protons, χ^{ss} is confined to right-handed chirality, i.e., a positive value near +90° (Schmidt et al., 1991). In the protonated form, long-range interactions between the Cys^1 and Cys^6 residues were not visible, except for that between the CH^{α} protons of the Cys^1 and Cys^6 residues, possibly due to overlap with intense short-range interactions. Similarly, only the NOE between Cys^6 CH^{α} and one of the Cys^1 CH^{β} protons was observed in the unprotonated form, agreeing with the calculated result of right-handed chirality, +70 ± 3°. In many proteins the value of the χ^{ss} angle is ±90 ± 15° (Richardson, 1981). Therefore, observation of a χ^{ss} angle of +42 ± 15° suggests that conformational averaging is probable in the protonated form, but in the unprotonated form there is a single main conformation that is consistent with experimental NOEs.

In the unprotonated form, no temperature dependence was observed for Tyr^2 NH and Asn^5 NH, suggesting that these protons either take part in intramolecular hydrogen bonds or are not

Ramachandran plots for the backbone dihedral angles, ϕ and ψ (Ramachandran and Sasisekharan, 1968), of five residues (except Cys^1) in the cyclic moiety for the 10 selected conformations of the two forms of oxytocin are shown in Fig. 6 (the ● marks show our data). In both forms angle variations occurred, but the angles for all residues can be grouped into a single conformation. The conformations for the Cys^1 and Tyr^2 residues were different between the two forms (Figs. 6A and C). The ϕ angles of Cys^1 were widely distributed, due to free rotation of the N-terminal protons, whereas the ψ angles were largely different between the two forms, $-175 \pm 4°$ for the protonated form and $+86 \pm 4°$ for the unprotonated form. The ϕ angle of Tyr^2 differed by 50° between the two forms. All ϕ angles for the endocyclic residues of calculated structures agree well with the experimental values, obtained from $^3J_{NH\text{-}CH\alpha}$ coupling constants (Table 2). The ϕ and ψ angles of the two β-turn corner residues at positions 3 and 4, which characterize the type of turn, are shown in Figs. 6B and D. The β-turn geometries were similar between the two forms. As for the ring closure, different mean S-S dihedral angles (χ^{ss}) for the calculated structures were obtained, $+70 \pm 3°$ for the unprotonated form and $+42 \pm 15°$ for the protonated form.

All of the side-chain χ^1 angles for the endocyclic residues of calculated structures roughly agree with the rotamer assignments, independently obtained from homo- and heteronuclear three-bond coupling constants for both forms (Table 1).

DISCUSSION

It has been suggested that oxytocin at high concentration in DMSO solution shows intermolecular interactions, leading to molecular association (Meraldi and Hruby, 1976). One goal of our study was to determine solution structures of oxytocin, based on distance analysis and hence investigate the possibility that oxytocin aggregates. First, we found no change in the proton chemical shifts observed at concentrations between 0.04 and 20.0 mM, although the line widths increased near 20 mM for both the protonated and unprotonated forms of oxytocin. Differences occurred, however, in the number of observed NOEs between the two forms. Besides the commonly observed NOEs, extra NOEs were obtained in the unprotonated form, which may possibly be interpreted as a result of specific intermolecular association or aggregation, driven by discharging at the N-terminus. The experimental cross-relaxation rates and calculated distances for backbone proton pairs in the cyclic moiety allow an estimate of the rotational correlation times, and hence the molecular weights for the two forms of oxytocin. If we assume an isotropic correlation time, τ_c, for each proton-spin pair i and j, the cross-relaxation rate can be determined as shown in Eq. 3 in Madrid et al. (1991). Using the experimental σ_{ij} and calculated r_{ij} of the 12 backbone proton pairs, τ_c values were obtained for each form of oxytocin. These τ_c values were determined to be 4.5×10^{-10} s (within an accuracy of 1%), irrespective of the state of the N-terminus. Having the same τ_c value among the 12 proton pairs is consistent with the assumption of a single peptide conformation. The presence of the same τ_c for either form of oxytocin verifies that there is only a minor change in conformation, excluding the possibility of an aggregation-state change upon protonation. The molecular weight of the peptide, roughly estimated from the Stokes–Einstein relation (Tanford, 1961) by assuming a spherical geometry, was about 800, in agreement with the monomer molecular weight of 1000 (Inoue and Akasaka, 1987).

We assumed a single, fairly restricted conformation, consistent with experimental NOE data.

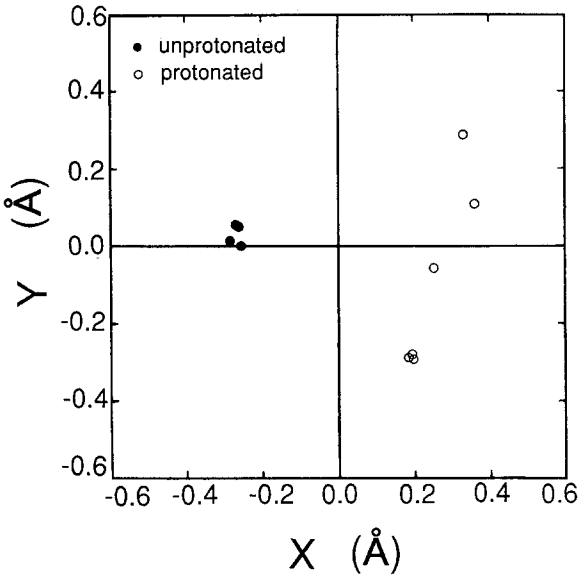

Fig. 8. Principal value analysis for the dispersion among 20 conformations (10 for unprotonated and 10 for protonated oxytocin), referenced to the backbone atoms in the cyclic part. The X and Y axes are arbitrary, corresponding to the first and second principal values.

shown in Figs. 6C and D (⊠ indicates the ϕ and ψ angles of the X-ray structures). In the crystal of deaminooxytocin, there were at least two possible conformations with different S-S dihedral chiralities, resulting in values of +76° with right-handed chirality and −101° with left-handed chirality (Wood et al., 1986). The ϕ and ψ angles for Tyr^2, Asn^5 and Cys^6 were similar for the solution and crystal structures, although those for Ile^3 and Gln^4 were significantly different, showing a type-II β-turn conformation. The ψ angles for Cys^1 (+86 ± 4°) and χ^{ss} (+70 ± 3°) in the unprotonated form were similar to those for one of the conformers of the crystal structures (+101° and +76°, respectively).

Recently, Bhaskaran et al. (1992) reported another conformation for oxytocin in DMSO, using restrained molecular dynamics. Their calculated conformations, which had a type-II β-turn, were different from the ones we determine here. The reasons for the difference might be attributed as follows. First, their calculation included an empirical energy function. Second, their conformation was derived based on a rigid model, where some of the distance constraints appeared to be too short compared to distances listed in the literature. Third, they did not obtain stereospecific assignments for the side-chain protons.

For a small peptide such as oxytocin (MW about 1000), problems of molecular flexibility or multiple conformers are very serious. For [Arg^8]vasopressin in DMSO, NMR parameters could be explained by taking into account rapid interconversion between different β-turn geometries in the tocin ring moiety, which consists of the sequence Tyr-Phe-Gln-Asn (Schmidt et al., 1991). There are many approaches that take the dynamical nature of peptides into account (Pearlman and Kollman, 1991), however, discussions are still going on about which approach would be most appropriate and how one could correctly assess the dynamical properties of molecules. The oxytocin showed rather rigid structures in DMSO, as judged from a large number of NOE peaks

in spite of the low molecular weight of the molecule (i.e., 14 NOEs/residue for the cyclic part). Therefore, we can safely claim that the approach established for determination of protein solution structures can be employed to this peptide sample. The χ^{ss} angle of about 45° for the protonated form was interpreted as the result of conformational averaging of two or more conformers. To confirm that no single conformation was consistent with all experimental NOEs, especially in the protonated form, we need to pursue a detailed study on the conformations of the two forms of oxytocin by using advanced conformational analysis, applying time- or ensemble-averaged molecular dynamics (Pearlman and Kollman, 1991).

CONCLUSIONS

Using several 2D NMR techniques, we obtained complete assignments of the ^{1}H and ^{13}C resonances for two forms of oxytocin, protonated and unprotonated at the N-terminal amino group in DMSO. Small but clear differences in many NMR parameters, such as J coupling constants and NOEs, were observed between the two forms. Distance analysis calculations in the dihedral-angle space, based on a relaxation matrix obtained from quantitative NOE intensities, showed that the overall structures with the lowest target functions were similar between the two forms, having a β-turn structure at the endocyclic residues Tyr-Ile-Gln-Asn. The local backbone conformations near the N-terminus, however, were noticeably different between the two forms. This is due to a change in the χ^{ss} dihedral angle, which closes the ring in the cyclic peptide. The differences in the NMR parameters can be attributed to not only an inductive effect of the N-terminal protonation but also to a change in conformation or conformational averaging. That is, in the unprotonated form, a single conformation is consistent with our distance analysis based on NOE constraints, but no single conformation is consistent with the distance analysis in the protonated form.

ACKNOWLEDGEMENTS

We thank Dr. Y. Kuroda at Protein Engineering Research Institute for useful discussions on the treatment of NMR data, and we also thank Drs. M. Fujiwara and R. Ishima at Biometrology Laboratory, JEOL, for helpful discussions. We are indebted to Mr. Y. Nakagawa at Peptide Institute, Inc., for contributing the valuable oxytocin hydrochloride and for useful suggestions.

REFERENCES

Bax, A., Griffey, R.H. and Hawkins, B.L. (1983) *J. Magn. Reson.*, **55,** 301–315.
Bax, A. and Summers, M.F. (1986) *J. Am. Chem. Soc.*, **108**, 2093–2094.
Bhaskaran, R., Chuang, L.-C. and Yu, C. (1992) *Biopolymers,* **32,** 1599–1608.
Braun, W. and Gō, N. (1985) *J. Mol. Biol.*, **186,** 611–626.
Braun, W., Bösch, C., Brown, L.R., Gō, N. and Wüthrich, K. (1981) *Biochim. Biophys. Acta,* **667,** 377–396.
Brewster, A.I.R., Glasel, J.A. and Hruby, V.J. (1972) *Proc. Natl. Acad. Sci. USA,* **69,** 1470–1474.
Brewster, A.I.R., Hruby, V.J., Spatola, A.F. and Bovey, F.A. (1973a) *Biochemistry,* **12,** 1643–1649.
Brewster, A.I.R., Hruby, V.J., Glasel, J.A. and Tonelli, A.E. (1973b) *Biochemistry,* **12,** 5294–5304.
Dorman, D.E. and Bovey, F.A. (1973) *J. Org. Chem.*, **38,** 2379–2383.
Deslauriers, R., Walter, R. and Smith, I.C.P. (1972) *Biochem. Biophys. Res. Commun.*, **48,** 854–859.

Deslauriers, R., Walter, R. and Smith, I.C.P. (1974) *Proc. Natl. Acad. Sci. USA,* **71,** 265–268.
Endo, S., Wako, H., Nagayama, K. and Gō, N. (1991) In *Computational Aspects of the Study of Biological Macromolecules by Nuclear Magnetic Resonance Spectroscopy* (Eds, Hoch, J.C., Poulsen, F.M. and Redfield, C.) Plenum Press, New York, pp. 233–251.
Ferrier, B.M., Jarvis, D. and Du Vigneaud, V. (1965) *J. Biol. Chem.*, **240,** 4264–4266.
Glickson, J.D., Urry, D.W., Havran, R.T. and Walter, R. (1972) *Proc. Natl. Acad. Sci. USA,* **69,** 2136–2140.
Glickson, J.D. (1975) In *Peptides; Chemistry, Structure, Biology* (Eds, Walter, R. and Meienhofer, J.) Ann Arbor Scientific Publications, Ann Arbor, pp. 787–802.
Güntert, P., Qian, Y.Q., Otting, G., Müller, M., Gehring, W. and Wüthrich, K. (1991) *J. Mol. Biol.,* **217,** 531–540.
Hansen, P.E. (1991) *Biochemistry,* **30,** 10457–10466.
Hendrickson, W.A. and Wüthrich, K. (1992) *Macromolecular Structures,* Current Biology Ltd., London, pp. 2–285.
Hofmann, M., Gehrke, M., Bermel, W. and Kessler, H. (1989) *Magn. Reson. Chem.,* **27,** 877–886.
Honig, D., Katat, E.A., Katz, L., Levinthal, D. and Wu, T.T. (1973) *J. Mol. Biol.,* **80,** 277–295.
Hruby, V.J., Deb, K.K., Fox, J., Bjarnason, J. and Tu, A.T. (1978) *J. Biol. Chem.,* **253,** 6060–6067.
Inoue, T. and Akasaka, K. (1987) *J. Biochem.,* **102,** 1371–1378.
Jeener, J., Meier, B.H., Bachmann, P. and Ernst, R.R. (1979) *J. Chem. Phys.,* **71,** 4546–4553.
Johnson, L.F., Schwartz, I.L. and Walter, R. (1969) *Proc. Natl. Acad. Sci. USA,* **64,** 1269–1275.
Kessler, H., Griesinger, C. and Wagner, K. (1987) *J. Am. Chem. Soc.,* **109,** 6927–6933.
Kumar, A., Ernst, R.R. and Wüthrich, K. (1980) *Biochem. Biophys. Res. Commun.,* **95,** 1–6.
Lewis, P.N., Momany, F.A. and Scheraga, H.A. (1973) *Biochim. Biophys. Acta,* **303,** 211–229.
Macura, S. and Ernst, R.R. (1980) *Mol. Phys.,* **41,** 95–117.
Madrid, M., Llinás, E. and Llinás, M. (1991) *J. Magn. Reson.,* **93,** 329–346.
Meraldi, J.-P. and Hruby, V.J. (1976) *J. Am. Chem. Soc.,* **98,** 408–410.
Molday, R.S., Englander, S.W. and Kallen, R.G. (1972) *Biochemistry,* **11,** 150–158.
Müller, L. (1987) *J. Magn. Reson.,* **72,** 191–196.
Nakai, T., Kidera, A. and Nakamura, H. (1993) *J. Biomol. NMR,* **3,** 19–40.
Neuhaus, D., Wagner, G., Wüthrich, K., Vašák, M. and Kägi, J.H.R. (1985) *Eur. J. Biochem.,* **151,** 257–273.
Pearlman, D.A. and Kollman, P.A. (1991) *J. Mol. Biol.*, **220,** 457–479.
Pratum, T.K., Hammen, P.K. and Andersen, N.H. (1988) *J. Magn. Reson.,* **78,** 376–381.
Ramachandran, G.N. and Sasisekharan, V. (1968) *Adv. Protein Chem.,* **23,** 283–437.
Rance, M., Sørensen, O.W., Bodenhausen, G., Wagner, G., Ernst, R.R. and Wüthrich, K. (1983) *Biochem. Biophys. Res. Commun.,* **117,** 479–485.
Richardson, J.S. (1981) *Adv. Protein Chem.,* **34,** 167–339.
Schmidt, J.M., Ohlenschläger, O., Rüterjans, H., Grzonka, Z., Kojro, E., Pavo, I. and Fahrenholz, F. (1991) *Eur. J. Biochem.,* **201,** 355–371.
Sheinblatt, M. (1966) *J. Am. Chem. Soc.,* **88,** 2123–2126.
Tanford, C. (1961) *Physical Chemistry of Macromolecules,* Wiley, New York.
Thomas, W.A. and Williams, M.K. (1972) *J. Am. Chem. Soc., Chem. Commun.,* 994.
Urry, D.W., Ohnishi, M. and Walter, R. (1970) *Proc. Natl. Acad. Sci. USA,* **66,** 111–115.
Urry, D.W. and Walter, R. (1971) *Proc. Natl. Acad. Sci. USA,* **68,** 956–958.
Wagner, G., Braun, W., Havel, T.F., Schaumann, T., Gō, N. and Wüthrich, K. (1987) *J. Mol. Biol.,* **196,** 611–639.
Walter, R., Glickson, J.D., Schwartz, I.L., Havran, R.T., Meienhofer, J. and Urry, D.W. (1972) *Proc. Natl. Acad. Sci. USA,* **69,** 1920–1923.
Walter, R., Smith, I.C.P. and Deslauriers, R. (1974) *Biochem. Biophys. Res. Commun.,* **58,** 216–221.
Walter, R., Wyssbrod, H.R. and Glickson, J.D. (1977) *J. Am. Chem. Soc.,* **99,** 7326–7332.
Wilmot, C.M. and Thornton, J.M. (1990) *Protein Eng.,* **3,** 479–493.
Wood, S.P., Tickle, I.J., Treharne, A.M., Pitts, J.E., Mascarenhas, Y., Li, J.Y., Husain, J., Cooper, S., Blundell, T.L., Hruby, V.J., Buku, A., Fischman, A.J. and Wyssbrod, H.R. (1986) *Science,* **232,** 633–636.
Wüthrich, K., Tun-kyi, A. and Schwyzer, R. (1972) *FEBS Lett.,* **25,** 104–108.
Wüthrich, K. (1986) *NMR of Proteins and Nucleic Acids,* Wiley, New York, pp. 117–161.